Available online at www.sciencedirect.com
SCIENCE DIRECT®
Solid-State Electronics 49 (2005) 889–895
SOLID-STATE ELECTRONICS
www.elsevier.com/locate/sse

An electron mobility model for wurtzite GaN

Frank Schwierz *

Fachgebiet Festkörperelektronik, Technische Universität Ilmenau, PF 100565, 98684 Ilmenau, Germany

Received 17 May 2004; received in revised form 9 February 2005; accepted 6 March 2005
Available online 21 April 2005

The review of this paper was arranged by Prof. S. Cristoloveanu

Abstract

A comprehensive model for the electron mobility in wurtzite (hexagonal) GaN is developed. A large number of experimental mobility data and the results of Monte Carlo transport simulations reported in the literature have been evaluated and serve as the basis for the model development. The proposed model describes the dependence of the mobility on carrier concentration, temperature, and electric field. Good agreement between the modeled low-field mobility and measured data at both room and elevated temperatures has been obtained. The Monte Carlo results of the high-field transport are correctly reproduced by the model. The model can be easily incorporated into numerical device simulators.

PACS: 72.20.Fr; 72.20.Ht

Keywords: Carrier mobility; Electron mobility; Mobility model; Device modeling; Simulation; Gallium nitride

1. Introduction

In recent years gallium nitride (GaN) has attracted a lot of attention. The properties of GaN make it a promising material for a variety of different electronic and optoelectronic devices. GaN has a wide direct bandgap of 3.4 eV and a resulting high breakdown field. Furthermore, it shows high peak and saturated electron drift velocities combined with a fairly high mobility. GaN appears in either the wurtzite (hexagonal) or the zincblende (cubic) crystal structure. While both GaN phases have been intensively investigated, currently wurtzite GaN is of primary importance for electron devices. Blue light emitting diodes and lasers based on GaN have been investigated intensively and became commercially available recently [1,2]. Experimental GaN-based high electron mobility transistors (HEMTs) clearly outperform all other types of field-effect transistors in terms of output power density at GHz frequencies [3] and show frequency limits f_T (cutoff frequency) and f_{max} (maximum frequency of oscillation) far above 100 GHz [4,5]. GaN metal-semiconductor field-effect transistors (MESFETs) with impressing high-frequency performance have been reported as well [6,7]. Recently also GaN-based sensors have been investigated [8].

Given the growing importance of GaN, reliable mobility models are urgently needed for device simulation and simulation-based optimization of device structures. Although lots of experimental mobility data is available in the technical literature and theoretical results on the carrier mobility have been published by several research groups, there is a lack of reliable mobility models suited for device simulation.

Two electron mobility models for GaN for use in device simulators have been reported recently [9,10]. The model from [9] is based on experimental mobility data

* Tel.: +49 3677 69 3120; fax: +49 3677 69 3132.
E-mail address: frank.schwierz@tu-ilmenau.de

0038-1101/$ - see front matter © 2005 Elsevier Ltd. All rights reserved.
doi:10.1016/j.sse.2005.03.006

collected from the technical literature (published in the period from 1973–1996) and allows to calculate the electron low-field mobility depending on carrier concentration and temperature. The decrease of the low-field mobility at low temperatures is described quite good, whereas the modeled mobility above room temperature shows deviations from measured data. Unfortunately, high-field transport is not considered by this model.

Farahmand et al. developed a mobility model based on the results of Monte Carlo transport simulations [10]. This model permits the calculation of the electron mobility depending on electron concentration, temperature, and field. The model is based entirely on theoretical results and the low-field mobility is overestimated especially for high carrier densities, i.e., high doping concentrations. The temperature dependence of the high-field mobility is described properly only for temperatures not much above room temperature. For high-power transistors, however, particularly the mobility at temperatures considerably higher than 300 K is of interest.

The aim of this paper is to provide an analytical model for the electron mobility in wurtzite GaN for use in device simulators. The new model goes beyond the previously published models from [9,10] since (a) new recently published mobility data are included in the model development, and (b) the temperature dependence of both the low-field and high-field mobilities at temperatures above room temperature is described more correctly. The present model is based on reported mobility data and includes the dependence of the mobility on doping concentration, temperature, and electric field. In the next section, our approach of mobility modeling is described. The model development and the results are presented in Section 3. Section 4 discusses the mobility model and Section 5 concludes the paper.

2. The approach of mobility modeling

In developing the GaN mobility model we closely follow the approach described in detail for SiC in [11]. The electron transport caused by an electric field E is described according to

$$v = \mu \times E \tag{1}$$

where v is the electron drift velocity and μ is the electron mobility. At low electric fields the electron velocity increases almost linearly with field and the mobility has the constant value μ_0 (low-field mobility). The low-field mobility depends on the electron concentration n, which in turn is a measure for the doping concentration, on the temperature T, and on the material quality. A widely used empirical expression for modeling the dependence of the low-field mobility on the electron concentration has been proposed by Caughey and Thomas [12]:

$$\mu_0 = \mu_{\min} + \frac{\mu_{\max} - \mu_{\min}}{1 + \left(\frac{n}{n_{\text{ref}}}\right)^{\alpha}} \tag{2}$$

where $\mu_{\min}$, $\mu_{\max}$, n_{ref} and α are fitting parameters. The parameter $\mu_{\max}$ represents the mobility of undoped or unintentionally doped samples, where lattice scattering is the main scattering mechanism, while $\mu_{\min}$ is the mobility in highly doped material, where impurity scattering is dominant. The parameter α is a measure of how quickly the mobility changes from $\mu_{\min}$ to $\mu_{\max}$ and n_{ref} is the carrier concentration at which the mobility is half way between $\mu_{\min}$ and $\mu_{\max}$. GaN is typically grown on sapphire, SiC, or Si substrates. This may lead to relatively high dislocation densities in the grown GaN layers. Especially in layers with low electron densities dislocation scattering affects the low-field mobility [13].

The temperature dependence of the low-field mobility can be modeled by making the four fitting parameters from Eq. (2) temperature dependent according to

$$\text{Par}(T) = \text{Par}_0 \times \left(\frac{T}{300\ \text{K}}\right)^{\gamma(\text{Par})} \tag{3}$$

where Par is the parameter of interest (i.e., $\mu_{\min}$, $\mu_{\max}$, n_{ref}, or α) and Par_0 is the value of the parameter Par at room temperature, i.e., at 300 K [14].

Under the influence of high electric fields, the electron velocity is no longer linearly dependent on the field. Instead, the relation between velocity and field has to be described by a mobility depending on the field. The field-dependent mobility $\mu(E)$ can be converted to the more frequently used field-dependent velocity $v(E)$ by

$$v(E) = \mu(E)E \tag{4}$$

The graphical representation of Eq. (4) is the stationary velocity-field characteristics. For Si and other materials showing a soft saturation behavior, the field dependence of the velocity can be modeled by the well established expression [15]

$$v = \frac{\mu_0 E}{\left(1 + \left(\frac{\mu_0 \times E}{v_{\text{sat}}}\right)^{\beta}\right)^{\frac{1}{\beta}}} \tag{5}$$

where v_{sat} and β are fitting parameters. Unfortunately, Eq. (5) is not suited for modeling the electron mobility at high-fields in GaN. Like GaAs and other III–V compounds, the velocity-field characteristics of GaN shows a pronounced peak and a region of negative differential mobility. An expression suited to model such velocity-field characteristics is [10]

$$v(E) = \frac{\mu_0 E + v_{\text{sat}}(E/E_c)^{n_1}}{1 + (E/E_c)^{n_1} + n_2(E/E_c)^{n_3}} \tag{6}$$

with μ_0 being the low-field mobility which depends on carrier concentration and temperature according to Eqs. (2) and (3), and v_{sat}, E_c, n_1, n_2 and n_3 are fitting

parameters. Up to now, the low-field mobility is the only quantity at the RHS of Eq. (6) showing a temperature dependence. This it not sufficient to properly model the temperature dependence of the velocity-field characteristics. Thus a temperature dependence of the fitting parameters is introduced by

$$\mathrm{Par}(T) = \mathrm{Par}_0 \times \left(a + bT + cT^2\right) \tag{7}$$

where Par is the parameter of interest (v_{sat}, E_c, n_1, n_2 n_3) and a, b, and c are constants that have to be determined by fitting.

In creating the models, the logical place to start was with the low-field mobility at 300 K, and to treat the further adaptions to the mobility model, i.e., temperature dependence and high-field mobility, as extensions to this. To get a data base for determining the various fitting parameters both measured mobility data and results of MC calculations have been compiled from the literature [16].

3. Model development

3.1. Room-temperature low-field mobility

Fig. 1 shows the experimental low-field mobilities (taken from a total of 30 Ref. [16]) used for the model development as a function of electron concentration. Different symbols are used for the results published by the end of 1996 and for those reported since early 1997 to show the progress obtained in the quality of epitaxially grown GaN, especially of reduced dislocation density, during the last 8 years. Dislocation scattering is a major source of mobility degradation in samples with low carrier densities. The high mobilities in excess of 1000 cm^2/V s reported recently for samples with carrier densities below 10^{17} cm^{-3} [17–22] are a result of the improved layer quality and the decreased dislocation density. Although the improved mobilities for samples with carrier densities below 10^{17} cm^{-3} are most impressive, it can be seen from Fig. 1 that also for samples with higher carrier densities up to 10^{19} cm^{-3} enhanced mobilities have been reported since 1997. It should be noted that the high mobilities mentioned above have been reported by several groups using different growing techniques. By the late 1990s the highest mobilities have been obtained in samples grown by hydride vapor phase epitaxy and metalorganic chemical vapor deposition. Meanwhile, however, GaN layers grown by molecular beam epitaxy showing competitive mobilities also have been reported (see, e.g. [20,22]).

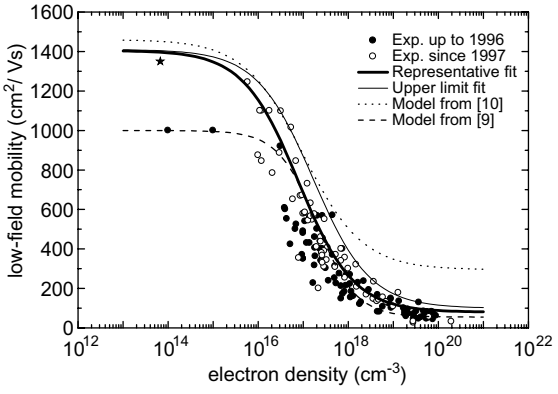

Fig. 1. Room-temperature low-field electron mobility as a function of electron concentration in GaN (perpendicular to the c-axis). Full circles: experimental data published by 1996; open circles: experimental data published since 1997; star: estimated maximum mobility in low-doped samples [17]; thick full line: representative mobility fit (this work); thin full line: upper limit mobility fit (this work); dashed line: calculated using the model from [9]; dotted line: calculated using the model from [10].

In the present work, two sets of fitting parameters have been elaborated. The first set, together with Eq. (2), results in what we call the representative fit. It models the typical mobilities expected from GaN samples, while the second set fits the best reported experimental results obtained so far (upper limit fit). Table 1 shows the parameter values obtained by fitting. The resulting dependences $\mu_0 = f(n)$ are shown in Fig. 1. Also included in the figure are the mobilities calculated using the mobility models proposed in [9,10] and an estimation of the maximum mobility in GaN samples with very low doping concentration [17]. Clearly the model from [9] predicts considerably lower mobilities for both very low and very high electron densities than the present model. The model from [10], on the other hand, overestimates the mobility for electron densities above 10^{18} cm^{-3} by a factor of 2–3.

3.2. Temperature-dependent low-field mobility

Compared to the mobility at room temperature, there is much less reported data on the electron mobility in GaN at elevated temperatures. For the model development, experimental data from [17,21,23–27] have been considered.

As seen in Fig. 1, the Caughey–Thomas fits do not pass exactly through all the relevant data points. It is very difficult to model any changes in mobility due to temperature, if the starting points (i.e., the mobilities at 300 K) do not match. Fortunately the temperature dependence is an exponential drop for temperatures above 300 K according to Eq. (3). It is thus possible to proportionally adjust the calculated mobilities to fit the experimental data at 300 K (by multiplying them with an adjustment factor C), without seriously changing the temperature dependence. The adjustment factor is calculated by

$$C = \frac{\mu_0(300\ \mathrm{K}, \mathrm{exp})}{\mu_0(300\ \mathrm{K}, \mathrm{mod})} \tag{8}$$

Table 1
Parameters for calculating the room-temperature low-field mobility using Eq. (2)

Type of fit	μ_{min}, $cm^2/V\,s$	μ_{max}, $cm^2/V\,s$	n_{ref}, $10^{17}\,cm^{-3}$	α
Representative fit	80	1405	0.778	0.71
Upper limit fit	100	1410	1.66	0.691

where μ_0 (300 K, exp) is the measured mobility at 300 K and μ_0 (300 K, mod) is the mobility calculated as described in Section 3.1. After performing this adjustment, the $(T/300\,K)^{\gamma}$ temperature dependences of the various parameters in the Caughey–Thomas equation were varied until reasonable agreement between the temperature dependent experimental mobilities and our fits had been obtained. The following temperature dependent parameters have been determined:

$$\gamma(\mu_{max}) = -2.85, \quad \gamma(\mu_{min}) = -0.2,$$
$$\gamma(n_{ref}) = 1.3, \quad \gamma(\alpha) = 0.31$$

In Fig. 2 the comparison between our fit and the measured temperature dependent mobilities from [17,21,23,24,26,27] is shown. It can be seen that the model reproduces the temperature dependence of the electron mobility in GaN quite well.

Fig. 3 shows a comparison of the mobilities predicted by the present model and by the models from [9,10] for a GaN sample with a electron concentration of $7 \times 10^{16}\,cm^{-3}$ together with the experimental results from [23] in the temperature range between 260 and 500 K. Since the three models result in different mobilities already at room temperature, the 300-K mobilities have been adjusted as described above. The present model shows very good agreement with the experiment. The model from [10] predicts a similar but slightly weaker temperature dependence of the mobility compared to the present model while the decrease of the mobility at elevated temperature is underestimated by the model from [9].

The majority of the experimental mobilities reported for $T > 300$ K follows the temperature dependence shown in Fig. 3. There are, however, some experimental results showing a slightly weaker temperature dependence.

3.3. High-field mobility

The modeling of the high-field mobility has been the most critical part of the entire model development. The base of experimental data for the high-field transport in GaN is quite limited. Only two reports on the measurement of the high-field mobility, i.e., the velocity-field characteristics, in GaN [28,29] have been published so far. Therefore, also the results of Monte Carlo transport simulations have been used to develop the model for the electron high-field mobility [10,30–34].

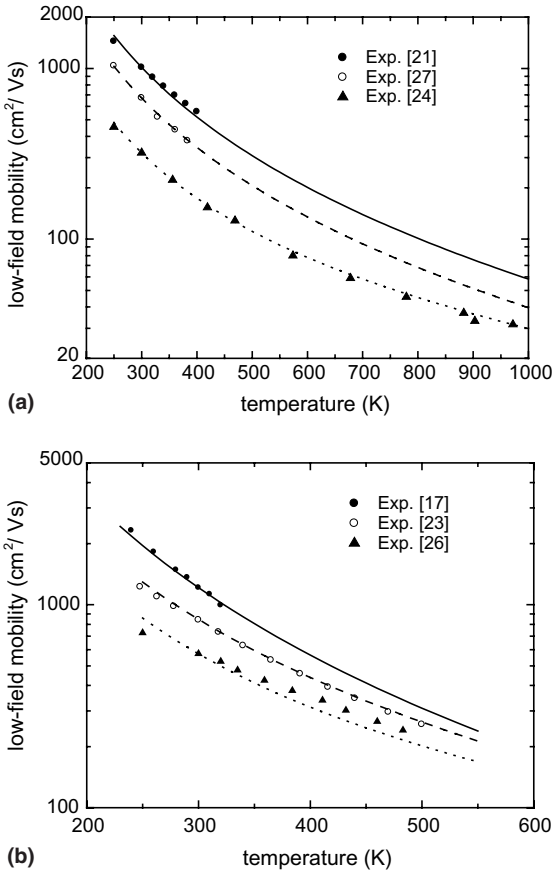

Fig. 2. Low-field electron mobility as a function of temperature in GaN. (a) Full circles and full line: experimental data from [21] and respective fit; open circles and dashed line: experimental data from [27] and respective fit; triangles and dotted line: experimental data from [24] and respective fit. (b) Full circles and full line: experimental data from [17] and respective fit; open circles and dashed line: experimental data from [23] and respective fit; triangles and dotted line: experimental data from [26] and respective fit.

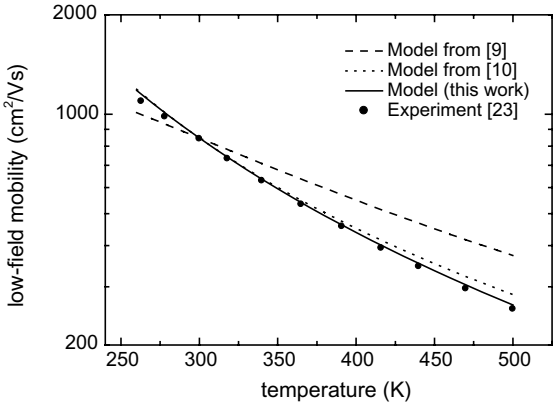

Fig. 3. Modeled low-field electron mobility in GaN as a function of temperature. Full line: present model; circles: experimental data from [23]; dotted line: calculated using the model from [10]; dashed line: calculated using the model from [9].

The experimental data and Monte Carlo results for 300 K shown in Fig. 4 constitute the data base for the

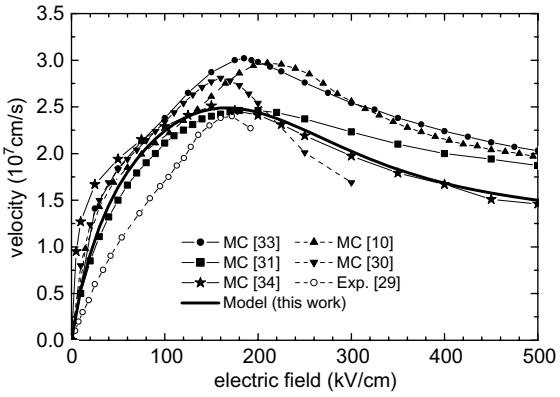

Fig. 4. Electron drift velocity at room temperature as a function of electric field in GaN. Circles, squares, and stars: Monte Carlo results from [10,30–34]; triangles: experimental data from [29]; thick full line: present model.

model development. Although the general shape of the velocity-field curves from the different references is similar, considerable quantitative differences can be observed. The measured peak velocities, for example, are much lower than those predicted by most of the Monte Carlo simulations. The maximum velocities in the experiments of Barker et al. [29] and Wraback et al. (not shown in the figure) [28] are only 2.4×10^7 cm/s and 1.9×10^7 cm/s, respectively, compared to around 3×10^7 cm/s calculated in [10,30,33]. Furthermore, the decline of the velocity at high-fields varies significantly. In a recent Monte Carlo study [34] electron–phonon interactions have been taken into account and a peak velocity of 2.5×10^7 cm/s (which is close to the measured 2.4×10^7 cm/s from [29]) as well as high-field velocities of $1.5–2\times10^7$ cm/s have been predicted. Because of the scattering of the experimental and Monte Carlo velocity-field data we did not try to get the best numerical fit but rather attempted to find a reasonable compromise between the mathematical fit, the theory-based expectations and the tendencies observed for the experimental and theoretical data.

The fitting procedure has been carried out as follows. The modeled 300-K low-field mobility (obtained by Eq. (2) applying the fitting parameters determined previously) has been fixed during fitting and the approximate value of the field at which the peak velocity occurs (around 200 kV/cm, see Fig. 4) has been taken as the initial value for the parameter E_c. Then by a fitting procedure the parameters v_{sat}, E_c, n_1, n_2 and n_3 from Eq. (6) have been ascertained. The following values have been obtained: $v_{sat} = 1.27\times10^7$ cm/s, $E_c = 172$ kV/cm, $n_1 = 4.19$, $n_2 = 3.24$, and $n_3 = 0.885$. The velocity-field characteristics calculated using Eq. (6) and the parameters given above is also shown in Fig. 4.

The final step was to include the temperature dependence of the high-field transport in the model. In [30,32,33] Monte Carlo transport simulations for temperatures ranging from 300 K to 1000 K have been carried out. The results of these calculations have been used to estimate the temperature dependence of the parameters v_{sat}, E_c, n_1, n_2, and n_3 according to Eq. (7). The obtained constants a, b, and c are shown in Table 2. To get an impression on how the proposed model describes the effect of elevated temperatures on the high-field transport, Fig. 5 shows the velocity-field characteristics calculated for GaN with an electron concentration of 10^{17} cm^{-3} for temperatures of 300 K, 450 K, and 600 K. The thick lines show the velocity-field characteristics calculated using the complete mobility model, i.e., we used Eq. (2) and the parameters from Table 1 for the room-temperature low-field mobility, Eq. (3) and the parameters $\gamma(\mu_{max})$, $\gamma(\mu_{min})$, $\gamma(n_{ref})$, and $\gamma(\alpha)$ given in Section 3.2 to model the low-field mobility at elevated temperature, and finally Eqs. (6) and (7) and the parameters from Table 2 for the high-field transport. The modeled velocity-field characteristics show the same trends as the Monte Carlo results from [30,32–34]. With increasing temperature

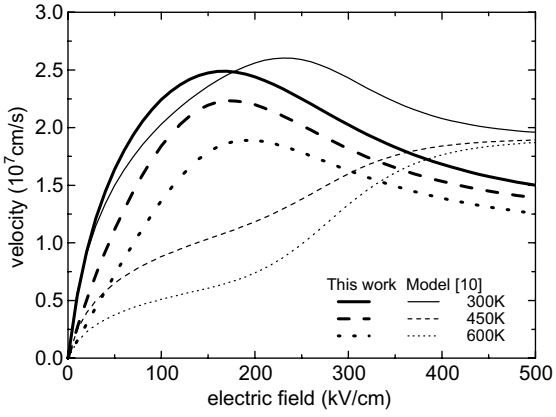

Fig. 5. Modeled electron drift velocity as a function of electric field for different temperatures. Thick lines: present model; thin lines: calculated using the model from [10].

Table 2
Parameters a, b, and c for the calculation of the temperature dependent values for v_{sat}, E_c, n_1, n_2, and n_3 using Eq. (7)

Par	v_{sat}	E_c	n_1	n_2	n_3
a	0.94475	0.8604	1.099	3.99	1.211
b, K^{-1}	5.5183×10^{-4}	3.88×10^{-4}	-3.1373×10^{-4}	-1.338×10^{-2}	-1.52×10^{-3}
c, K^{-2}	-1.2256×10^{-6}	2.5778×10^{-7}	-5.280×10^{-8}	1.1373×10^{-5}	2.727×10^{-6}

– the slope at low-fields, the peak velocity, and the velocity at high fields decrease;
– the electric field at which the peak velocity occurs increases.

Fig. 5 also shows the velocity-field characteristics calculated using the model from [10]. This model also applies Eq. (6). Contrary to the present model, however, only the low-field mobility is assumed to be temperature dependent, while the parameters v_{sat}, E_c, n_1, n_2, and n_3 are constant and do not vary with temperature. Clearly the high-field transport at elevated temperatures is not described correctly by the model from [10].

4. Discussion

In Eq. (2) of the present model, the low-field mobility is calculated as a function of the electron concentration. Instead of using the electron concentration it is also possible to employ other quantities, such as the absolute or ionized doping. Although the actual electron concentration may be somewhat different from the absolute or ionized doping in GaN, no significant difference in the modeled mobilities has been found. Since many published experimental mobility data refer to the electron concentration, in our model development the actual carrier concentration has been considered. Another important factor is the difference between the commonly reported Hall mobility and the drift mobility (i.e., the low-field mobility to be modeled). The conversion factor depends on the nature of the semiconductor as well as the setup used to measure the Hall mobility (particularly the magnetic field). It is usually not reported even if the laboratory in question is able to determine it. For that reason, in this work it is assumed to be unity.

The velocity-field characteristics have been modeled by Eq. (6) containing the low-field mobility μ_0 and the five fitting parameters v_{sat}, E_c, n_1, n_2, and n_3. The equation

$$v(E) = \frac{\mu_0 E + \mu_1 E (E/E_1)^{n_1} + v_{sat}(E/E_2)^{n_2}}{1 + (E/E_1)^{n_1} + (E/E_2)^{n_2}} \quad (9)$$

is an alternative expression that can be used to reproduce GaN velocity-field characteristics [35]. In Eq. (9), μ_0 is the low-field mobility and μ_1, v_{sat}, n_1, n_2, E_1, and E_2 are fitting parameters. Using Eq. (9) the velocity-field characteristics of GaN can be reproduced slightly better than with Eq. (6). Eq. (9) shows, however, some drawbacks. Compared to Eq. (6) it contains six fitting parameters that have to be determined instead of five. The parameter E_c in Eq. (6) is closely related to the field for the peak velocity. This fact makes the first estimate of E_c quite simple and is also helpful in the process of determining the temperature dependence of E_c. The parameters E_1 and E_2 from Eq. (9), on the other hand, are not related to a characteristic point of the velocity-field characteristics. Given the considerable scattering in the velocity-field data currently available, see Fig. 4, we decided to use the more simple expression, i.e., Eq. (6), in our model.

5. Conclusion

A comprehensive electron mobility model for bulk wurtzite (hexagonal) GaN has been developed. The model is based on a large number of experimental data and MC results published in the open literature. The new model describes the dependence of the mobility on electron concentration, temperature, and field quite well. It consists of simple analytical equations and can be easily incorporated in a numerical device simulator. Thus the presented mobility models can be used in device simulations to design and optimize different GaN device structures.

Acknowledgement

This work has been supported by Deutsche Forschungsgemeinschaft DFG under project no. Schw 729/2-3.

References

[1] Amano H, Kamiyama S, Akasaki I. Impact of low-temperature buffer layers on nitride-based optoelectronics. Proc IEEE 2002; 90:1015–21.
[2] Arakawa Y. Progress in GaN-based quantum dots for optoelectronic applications. IEEE J Sel Top Quantum Electron 2002; 8:823–32.
[3] Wu Y-F, Saxler A, Moore M, Smith RP, Sheppard S, Chavarkar PM, et al. 30-W/mm GaN HEMT by field plate optimization. IEEE Electron Dev Lett 2004;25:117–9.
[4] Kumar V, Lu W, Schwindt R, Kuliev A, Simin G, Yang J, et al. AlGaN/GaN HEMTs on SiC with f_T of over 120 GHz. IEEE Electron Dev Lett 2002;23:455–7.
[5] Quay R, Kiefer R, van Raay F, Massler H, Ramberger S, Müller S, et al. AlGaN/GaN HEMTs on SiC operating at 40 GHz. Tech Dig IEDM 2002:673–6.
[6] Gaska R, Shur MS, Hu X, Yang JW, Tarakji A, Simin G, et al. Highly doped thin-channel GaN-metal-semiconductor field-effect transistors. Appl Phys Lett 2001;78:769–71.
[7] Lee C, Lu W, Piner E, Adesida I. DC and microwave performance of recessed-gate GaN MESFETs using ICP-RIE. Solid-State Electron 2002;46:743–6.
[8] Eickhoff M, Schalwig J, Steinhoff G, Weidemann O, Görgens L, Neuberger R, et al. Electronics and sensors based on pyroelectric AlGaN/GaN heterostructures. Part B: Sensor applications. Phys Status Solidi (c) 2003;0:1908–18.
[9] Mnatsakanov TT, Levinshtein ME, Pomortseva LI, Yurkov SN, Simin GS, Khan MA. Carrier mobility model for GaN. Solid-State Electron 2003;47:111–5.
[10] Farahmand M, Garetto C, Belotti E, Brennan KF, Goano M, Ghillino E, et al. Monte Carlo simulation of electron transport

in the III-nitride wurtzite phase materials system: Binaries and ternaries. IEEE Trans Electron Dev 2001;48:535–42.
[11] Roschke M, Schwierz F. Electron mobility models for 4H, 6H, and 3C SiC. IEEE Trans Electron Dev 2001;48:1442–7.
[12] Caughey DM, Thomas RE. Carrier mobilities in silicon empirically related to doping and field. Proc IEEE 1967;52:2192–3.
[13] Eastman L, Chu K, Schaff W, Murphy M, Weimann NG, Eustis T. High-frequency AlGaN/GaN MODFETs. MRS Int J Nitride Semicond Res 1997;2, Article 17.
[14] Arora ND, Hauser JR, Roulston DJ. Electron and hole mobilities in silicon as a function of concentration and temperature. IEEE Trans Electron Dev 1982;29:292–5.
[15] Selberherr S. Analysis and simulation of semiconductor devices. Wien: Springer-Verlag; 1984.
[16] Schwierz F. Electron mobility in bulk GaN and in AlGaN/GaN 2DEGs: A compilation of more than 200 references. TU Ilmenau, 2004, unpublished.
[17] Look DC, Sizelove JR. Predicted maximum mobility in bulk GaN. Appl Phys Lett 2001;79:1133–5.
[18] Fang Z-Q, Look DC, Visconti P, Wang D-F, Lu C-Z, Morkoc H, et al. Deep centers in a free-standing GaN layer. Appl Phys Lett 2001;78:2178–80.
[19] Fong WK, Zhu CF, Leung BH, Surya C. High-mobility GaN epilayer grown by RF plasma-assisted molecular beam epitaxy on intermediate-temperature GaN buffer layer. J Cryst Growth 2001;233:431–8.
[20] Heying B, Smorchkova I, Poblenz C, Elsass C, Fini P, Den Baars S, et al. Optimization of the surface morphologies and electron mobilities in GaN grown by plasma-assisted molecular beam epitaxy. Appl Phys Lett 2000;77:2885–7.
[21] Look DC, Reynolds DC, Hemsky JW, Sizelove JR, Jones RL, Molnar RJ. Defect donors and acceptors in GaN. Phys Rev Lett 1997;79:2273–6.
[22] Tang H, Webb JB. Growth of high mobility GaN by ammonia-molecular beam epitaxy. Appl Phys Lett 1999;74:2373–4.
[23] Götz W, Romano LT, Walker J, Johnson NM, Molnar RJ. Hall-effect analysis of GaN films grown by hydride vapor phase epitaxy. Appl Phys Lett 1998;72:1214–6.
[24] Ilegems M, Montgomery HC. Electrical properties of n-type vapor-grown gallium nitride. J Phys Chem 1973;34:885–95.
[25] Khan MA, Kuznia JN, Van Hove JM, Olson DT, Krishnankutty S, Kolbas RM. Growth of high optical and electrical quality GaN layers using low-pressure metalorganic chemical vapor deposition. Appl Phys Lett 1991;58:526–7.
[26] Götz W, Johnson NM, Chen C, Liu H, Kuo C, Imler W. Activation energies of Si donors in GaN. Appl Phys Lett 1996; 68:3144–6.
[27] Eshghi H, Lancefield D, Beaumont B, Gibart P. Electron transport in MOVPE GaN grown on silicon nitride treated sapphire. Phys Status Solidi (b) 1999;216:733–6.
[28] Wraback M, Shen H, Carrano JC, Li T, Campbell JC, Schurman MJ, et al. Time-resolved electroabsorption measurement of the electron velocity-field characteristic in GaN. Appl Phys Lett 2000;76:1155–7.
[29] Barker JM, Akis R, Ferry DK, Goodnick SM, Thornton TJ, Koleske DD, et al. High-field transport studies of GaN. Physica B 2002;314:39–41.
[30] Mansour NS, Kim KW, Littlejohn MA. Theoretical study of electron transport in gallium nitride. J Appl Phys 1995;77: 2834–6.
[31] Kolnik J, Oguzman IH, Brennan KF, Wang R, Ruden PP, Wang Y. Electronic transport studies of bulk zincblende and wurtzite phases of GaN based on an ensemble Monte Carlo calculation including a full zone band structure. J Appl Phys 1995;78:1033–8.
[32] Bhapkar U, Shur MS. Monte Carlo calculation of velocity-field characteristics of wurtzite GaN. J Appl Phys 1997;82:1649–55.
[33] Albrecht JD, Wang RP, Ruden PP, Farahmand M, Brennan KF. Electron transport characteristics of GaN for high temperature device modeling. J Appl Phys 1998;83:4777–81.
[34] Yamakawa S, Aboud S, Saraniti M, Goodnick SM. Influence of the electron–phonon interaction on electron transport in wurtzite GaN. Semicond Sci Technol 2004;19:S475–7.
[35] Polyakov VM, Schwierz F. Influence of electron mobility modeling on DC *I–V* characteristics of WZ-GaN MESFETs. IEEE Trans Electron Dev 2001;48:512–6.